

NH-Tautomerization of 2-Substituted Pyridines and Quinolines on Osmium and Ruthenium: Determining Factors and Mechanism

Miguel A. Esteruelas,* Francisco J. Fernández-Alvarez, and Enrique Oñate

Departamento de Química Inorgánica, Instituto de Ciencia de Materiales de Aragón, Universidad de Zaragoza-CSIC, 50009 Zaragoza, Spain

Received August 13, 2008

Complexes $\text{MH}_2\text{Cl}_2(\text{P}^i\text{Pr}_3)_2$ ($\text{M} = \text{Os}$ (**1**), Ru (**1a**)) promote the NH-tautomerization of 2-methylpyridine and stabilize the resulting NH-tautomer to afford the dihydrogen derivatives $\text{MCl}_2(\eta^2\text{-H}_2)\{\kappa\text{-C-}[\text{HNC}_5\text{H}_3\text{Me}]\}(\text{P}^i\text{Pr}_3)_2$ ($\text{M} = \text{Os}$ (**2**), Ru (**3**)), containing the heterocycle coordinated by the C_α atom. In dichloromethane under reflux, complex **3** loses the coordinated hydrogen molecule to give the five-coordinate derivative $\text{RuCl}_2\{\kappa\text{-C-}[\text{HNC}_5\text{H}_3\text{Me}]\}(\text{P}^i\text{Pr}_3)_2$ (**4**). In contrast to 2-methylpyridine, the reactions of **1** and **1a** with pyridine lead to $\text{MCl}_2\{\kappa\text{-N-}[\text{NC}_5\text{H}_5]\}_3(\text{P}^i\text{Pr}_3)$ ($\text{M} = \text{Os}$ (**5**), Ru (**5a**)), containing the heterocycle coordinated by the lone pair of the nitrogen. DFT calculations using PMe_3 as a model of P^iPr_3 show that the formation of **2** and the related quinoline complex $\text{OsCl}_2(\eta^2\text{-H}_2)\{\kappa\text{-C-}[\text{HNC}_9\text{H}_6]\}(\text{P}^i\text{Pr}_3)_2$ (**6**) involves an intermolecular osmium to nitrogen hydrogen migration, the subsequent $\text{C}_\alpha\text{-H}$ bond activation of the protonated heterocycle, and the dihydride–dihydrogen tautomerization of the resulting dihydride. The structures of **2** and **5** have been determined by X-ray diffraction analysis.

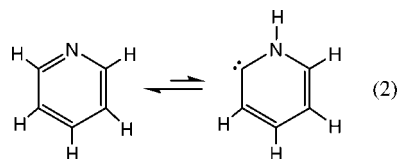
Introduction

Transition-metal elements have the remarkable ability to modify the chemical behavior of organic molecules. The metal-induced alkyne–vinylidene rearrangement is an attractive illustration. Although the activation energy for the acetylene–vinylidene isomerization (eq 1) is $76 \text{ kcal}\cdot\text{mol}^{-1}$ and the latter lies $44 \text{ kcal}\cdot\text{mol}^{-1}$ above the former in energy, numerous transition-metal vinylidene complexes have been reported in recent years.¹ Other tautomerizations or isomerizations of C–C and C–E ($\text{E} = \text{O}, \text{N}$) double bonds by a formal 1,2-hydrogen shift at a metal center are quite rare and hence less well investigated.²



Pyridines, which are extensively used in the pharmaceutical industry,³ have a ubiquitous presence in transition-metal chemistry. Their more classical mode of coordination is $\kappa\text{-N}$ via the lone pair of the nitrogen atom. Several alternative metal ligand interactions, including $\eta^2\text{-C,N-}$, $\eta^2\text{-C,C-}$, and η^6 -bound pyridine complexes, have been also documented.⁴ Like acetylene, pyridine has a less stable tautomer, which lies about $40 \text{ kcal}\cdot\text{mol}^{-1}$ above the usual one (eq 2).⁵ Although this NH-species was postulated almost 70 years ago⁶ and generated in the gas phase in 1996,^{5,7} the tautomerization of pyridine, 2-substituted pyridines, 2,2'-bipyridine, and 1,10-phenanthroline has been recently observed. Carmona and co-workers⁸ have

reported that $\text{Tp}^{\text{Me}_2}\text{Ir-complexes}$ ($\text{Tp}^{\text{Me}_2} = \text{hydrotris}(3,5\text{-dimethylpyrazolyl})\text{borate}$) promote the isomerization of these heterocycles and stabilize the corresponding NH-tautomers.



We have concurrently found the same type of tautomers for quinolines (eq 3).⁹ Complexes $\text{MH}_2\text{Cl}_2(\text{P}^i\text{Pr}_3)_2$ ($\text{M} = \text{Os}, \text{Ru}$) promote the tautomerization of quinoline, 8-methylquinoline, and benzo[*h*]quinoline to afford NH-tautomers, which are stabilized by coordination of the carbon atom at the α -position of the heterocycle to the metal center and by means of a

* Corresponding author. E-mail: maester@unizar.es.

(1) (a) Bruce, M. I. *Chem. Rev.* **1991**, *91*, 197. (b) Puerta, M. C.; Valerga, P. *Coord. Chem. Rev.* **1999**, *977*, 193–195. (c) Valyaev, D. A.; Semeikin, O. V.; Ustynyuk, N. A. *Coord. Chem. Rev.* **2004**, *248*, 1679. (d) Esteruelas, M. A.; López, A. M. *Organometallics* **2005**, *24*, 3584. (e) Esteruelas, M. A.; López, A. M.; Oliván, M. *Coord. Chem. Rev.* **2007**, *251*, 795.

(2) Kunz, D. *Angew. Chem., Int. Ed.* **2007**, *46*, 3405.

(3) Carey, J. S.; Laffan, D.; Thomson, C.; Williams, M. T. *Org. Biomol. Chem.* **2006**, *4*, 2337.

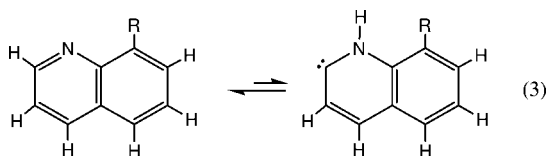
(4) (a) Cordone, R.; Taube, H. *J. Am. Chem. Soc.* **1987**, *109*, 8101. (b) Wucherer, E. J.; Muettterties, E. L. *Organometallics* **1987**, *6*, 1691. (c) Fish, R. H.; Kim, H.-S.; Fong, R. H. *Organometallics* **1989**, *8*, 1375. (d) Cordone, R.; Harman, W. D.; Taube, H. *J. Am. Chem. Soc.* **1989**, *111*, 2896. (e) Davies, S. G.; Shipton, M. R. *J. Chem. Soc., Chem. Commun.* **1989**, 995. (f) Strickler, J. R.; Bruck, M. A.; Wigley, D. E. *J. Am. Chem. Soc.* **1990**, *112*, 2814. (g) Covert, K. J.; Neithamer, D. R.; Zonneville, M. C.; La Pointe, R. E.; Schaller, C. P.; Wolczanski, P. T. *Inorg. Chem.* **1991**, *30*, 2494. (h) Smith, D. P.; Strickler, J. R.; Gray, S. D.; Bruck, M. A.; Holmes, R. S.; Wigley, D. E. *Organometallics* **1992**, *11*, 1275. (i) Harman, W. D. *Chem. Rev.* **1997**, *97*, 1953. (j) Kleckley, T. S.; Bennett, J. L.; Wolczanski, P. T.; Lobkovsky, E. B. *J. Am. Chem. Soc.* **1997**, *119*, 247. (k) Meiere, S. H.; Brooks, B. C.; Gunnoe, T. B.; Sabat, M.; Harman, W. D. *Organometallics* **2001**, *20*, 1038. (l) Meiere, S. H.; Brooks, B. C.; Gunnoe, T. B.; Carrington, E. H.; Sabat, M.; Harman, W. D. *Organometallics* **2001**, *20*, 3661. (m) Bonanno, J. B.; Veige, A. S.; Wolczanski, P. T.; Lobkovsky, E. B. *Inorg. Chim. Acta* **2003**, *345*, 173. (n) Ozerov, O. V.; Pink, M.; Watson, L. A.; Caulton, K. G. *J. Am. Chem. Soc.* **2004**, *126*, 2105. (o) Graham, P. M.; Delafuente, D. A.; Liu, W.; Myers, W. H.; Sabat, M.; Harman, W. D. *J. Am. Chem. Soc.* **2005**, *127*, 10568.

(5) Lavorato, D. J.; Terlouw, J. K.; Dargel, T. K.; Koch, W.; McGibbon, G. A.; Schwarz, H. *J. Am. Chem. Soc.* **1996**, *118*, 11898.

(6) Ashworth, M. R. F.; Daffern, R. P.; Hammick, D. L. *J. Chem. Soc.* **1939**, 809.

(7) Lavorato, D. J.; Terlouw, J. K.; McGibbon, G. A.; Dargel, T. K.; Koch, W.; Schwarz, H. *Int. J. Mass. Spectrom.* **1998**, *179–180*, 7.

Cl \cdots H–N interaction between the NH-hydrogen atom and a chloride ligand of the metal fragment. Whittlesey and co-workers¹⁰ have described ruthenium isomers resulting from the N- or C-bound tautomers of isopropyl-4,5-dimethylimidazole, in agreement with the possibility that C-bound imidazoles could have some role in metalloproteins chemistry.¹¹ During the last months, work has shown that other N-heterocycles can also undergo a metal-induced rearrangement to form N-heterocyclic carbene complexes.¹²



Intramolecular transfer of a proton in tautomeric systems is the key step in numerous important biological processes, where the energetically less stable tautomer is often an active intermediate, which dictates the mechanism and the formed product.¹³ The rearrangement of N-heterocycles is also important from the point of view of some relevant catalytic reactions¹⁴ and for the preparation of new materials.¹⁵ For instance, Bergman, Ellman, and co-workers have proposed that the C,N-1,2-hydrogen shift is the key step for the rhodium(I)-catalyzed *ortho* alkylation of pyridines and quinolines.^{14b,e} Stöhr, Jung, Gade, and co-workers have shown that thermally induced C–C coupling reactions of polycyclic heteroaromatic compounds may be used to generate electronically highly delocalized polyaromatic chains, via the tautomerization of the N-heterocyclic end units to carbene intermediates, which couple according to a Wanzlick-type dimerization.¹⁵

A rapid growth of the number of evidence showing the participation and significance of such tautomerizations in other fields can be advanced, as well as of the number of transition-metal complexes containing NH-tautomers. For instance, as a part of the work of our group on C–H bond activation reactions

promoted by osmium–polyhydride complexes,¹⁶ we have recently observed that the *ortho*-C–H bond activation of benzophenone by the hydride–dihydrogen derivative [OsH(η^2 -CH₂=CH-*o*-C₅H₄N)(P^{*i*}Pr₃)₂]BF₄ is accompanied with the tautomerization of 2-ethylpyridine. Furthermore, the retrotautomerization in the resulting compound [Os{C₆H₄C(O)}Ph](η^2 -H₂){ κ -C-[HNC₅H₃Et]}P^{*i*}Pr₃)₂]BF₄ is disfavored with regard to the elimination of the *ortho*-metalated ketone.¹⁷ In order to rationalize these types of processes, some knowledge about the mechanism of the C,N-1,2-hydrogen shift is now essential.

In this paper, we show that complexes MH₂Cl₂(P^{*i*}Pr₃)₂ (M = Os, Ru) also promote the tautomerization of 2-methylpyridine and stabilize the resulting tautomer, prove the importance of the substituent of the pyridine for the tautomerization process, and summarize the results of theoretical calculations on the mechanism of the tautomerization of pyridines and quinolines in the presence of OsH₂Cl₂(P^{*i*}Pr₃)₂.

Results and Discussion

1. Tautomerization of 2-Methylpyridine. Complex OsH₂Cl₂(P^{*i*}Pr₃)₂ (**1**) tautomerizes 2-substituted pyridines and stabilizes the corresponding NH-tautomers. Thus, the treatment of this compound with 8.0 equiv of 2-methylpyridine in toluene at 95 °C for 48 h leads to OsCl₂(η^2 -H₂){ κ -C-[HNC₅H₃-Me]}(P^{*i*}Pr₃)₂ (**2**), which is isolated as a yellow solid in 65% yield. In agreement with the trend shown by **1** to afford species with a nonclassical H–H interaction when a Lewis base is coordinated,¹⁸ the tautomerization and stabilization of the resulting heterocycle are accompanied with the transformation of the OsH₂-dihydride unit of the starting compound into elongated dihydrogen in **2** (eq 4).

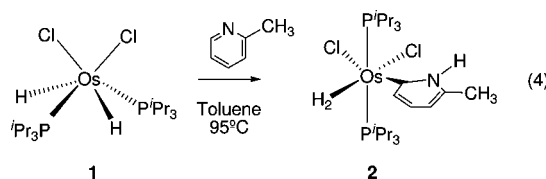


Figure 1 shows a view of the X-ray structure of **2**. The coordination geometry around the osmium atom can be rationalized as derived from a distorted octahedron with the phosphorus atoms of the triisopropylphosphine ligands occupying *trans* positions (P(1)–Os–P(2) = 170.79(7)°). The metal sphere is completed by the chloride ligands mutually *cis* disposed (Cl(1)–Os–Cl(2) = 87.18(7)°), the tautomerized 2-methylpyridine group *trans* disposed to Cl(2) (C(1)–Os–Cl(2) = 173.9(2)°), and the elongated dihydrogen ligand *trans* disposed

(8) (a) Alvarez, E.; Conejero, S.; Paneque, M.; Petronilho, A.; Poveda, M. L.; Serrano, O.; Carmona, E. *J. Am. Chem. Soc.* **2006**, *128*, 13060. (b) Alvarez, E.; Conejero, S.; Lara, P.; López, J. A.; Paneque, M.; Petronilho, A.; Poveda, M. L.; del Rio, D.; Serrano, O.; Carmona, E. *J. Am. Chem. Soc.* **2007**, *129*, 14130. (c) Conejero, S.; Lara, P.; Paneque, M.; Petronilho, A.; Poveda, M. L.; Serrano, O.; Vattier, F.; Alvarez, E.; Maya, C.; Salazar, V.; Carmona, E. *Angew. Chem., Int. Ed.* **2008**, *47*, 4380.

(9) (a) Esteruelas, M. A.; Fernández-Alvarez, F. J.; Oñate, E. *J. Am. Chem. Soc.* **2006**, *128*, 13044. (b) Esteruelas, M. A.; Fernández-Alvarez, F. J.; Oñate, E. *Organometallics* **2007**, *26*, 5239.

(10) Burling, S.; Mahon, M. F.; Powell, R. E.; Whittlesey, M. K.; Williams, J. M. J. *J. Am. Chem. Soc.* **2006**, *128*, 13702.

(11) Sini, G.; Eisenstein, O.; Crabtree, R. H. *Inorg. Chem.* **2002**, *41*, 602.

(12) (a) Ruiz, J.; Perandones, B. F. *J. Am. Chem. Soc.* **2007**, *129*, 9298. (b) Wang, X.; Chen, H.; Li, X. *Organometallics* **2007**, *26*, 4684. (c) Begum, R.; Komuro, T.; Tobita, H. *Chem. Lett.* **2007**, *36*, 650. (d) Gribble, M. W., Jr.; Ellman, J. A.; Bergman, R. G. *Organometallics* **2008**, *27*, 2152. (e) Araki, K.; Kuwata, S.; Ikariya, T. *Organometallics* **2008**, *27*, 2176.

(13) Raczynska, E. D.; Kosińska, W.; Osmialowski, B.; Gawinecki, R. *Chem. Rev.* **2005**, *105*, 3561.

(14) (a) Wiedemann, S. H.; Lewis, J. C.; Ellman, J. A.; Bergman, R. G. *J. Am. Chem. Soc.* **2006**, *128*, 2452. (b) Lewis, J. C.; Bergman, R. G.; Ellman, J. A. *J. Am. Chem. Soc.* **2007**, *129*, 5332. (c) Larivée, A.; Mousseau, J. J.; Charette, A. B. *J. Am. Chem. Soc.* **2008**, *130*, 52. (d) Nakao, Y.; Kanyiva, K. S.; Hiyama, T. *J. Am. Chem. Soc.* **2008**, *130*, 2448. (e) Lewis, J. C.; Berman, A. M.; Bergman, R. G.; Ellman, J. A. *J. Am. Chem. Soc.* **2008**, *130*, 2493.

(15) Matena, M.; Riehm, T.; Stöhr, M.; Jung, T. A.; Gade, L. H. *Angew. Chem., Int. Ed.* **2008**, *47*, 2414.

(16) See for example: (a) Eguillor, B.; Esteruelas, M. A.; Oliván, M.; Oñate, E. *Organometallics* **2005**, *24*, 1428. (b) Esteruelas, M. A.; Hernández, Y. A.; López, A. M.; Oliván, M.; Oñate, E. *Organometallics* **2005**, *24*, 5989. (c) Esteruelas, M. A.; Fernández-Alvarez, F. J.; Oliván, M.; Oñate, E. *J. Am. Chem. Soc.* **2006**, *128*, 4596. (d) Esteruelas, M. A.; Hernández, Y. A.; López, A. M.; Oliván, M.; Oñate, E. *Organometallics* **2007**, *26*, 2193. (e) Baya, M.; Eguillor, B.; Esteruelas, M. A.; Lledós, A.; Oliván, M.; Oñate, E. *Organometallics* **2007**, *26*, 5140. (f) Esteruelas, M. A.; Hernández, Y. A.; López, A. M.; Oliván, M.; Rubio, L. *Organometallics* **2008**, *27*, 799. (g) Esteruelas, M. A.; Masamunt, A. B.; Oliván, M.; Oñate, E.; Valencia, M. *J. Am. Chem. Soc.* **2008**, *130*, 11612.

(17) (a) Buil, M. L.; Esteruelas, M. A.; Garcés, K.; Oliván, M.; Oñate, E. *J. Am. Chem. Soc.* **2007**, *129*, 10998. (b) Buil, M. L.; Esteruelas, M. A.; Garcés, K.; Oliván, M.; Oñate, E. *Organometallics* **2008**, *27*, 4680.

(18) (a) Esteruelas, M. A.; Oro, L. A.; Ruiz, N. *Inorg. Chem.* **1993**, *32*, 3793. (b) Esteruelas, M. A.; Lahoz, F. J.; Oro, L. A.; Oñate, E.; Ruiz, N. *Inorg. Chem.* **1994**, *33*, 787. (c) Barea, G.; Esteruelas, M. A.; Lledós, A.; López, A. M.; Tolosa, J. I. *Inorg. Chem.* **1998**, *37*, 5033.

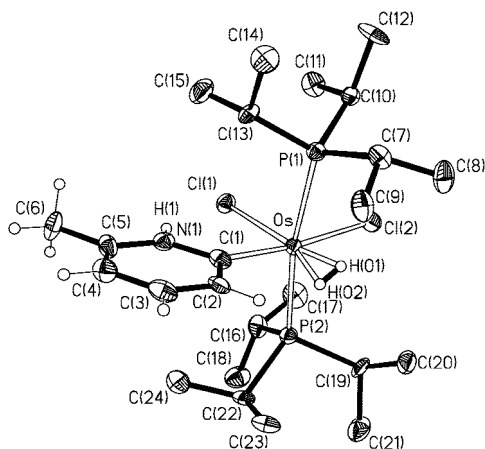


Figure 1. Molecular diagram of complex **2**. Selected bond lengths (Å) and angles (deg): Os–C(1) = 2.055(8), Os–Cl(1) = 2.4903(19), Os–Cl(2) = 2.5067(19), Os–P(1) = 2.409(2), Os–P(2) = 2.404(2), C(1)–N(1) = 1.366(9), C(5)–N(1) = 1.386(10), C(1)–C(2) = 1.411(10), C(2)–C(3) = 1.372(11), C(3)–C(4) = 1.388(11), C(4)–C(5) = 1.351(11), Cl(1)···H(1)N = 2.14(11); P(1)–Os–P(2) = 170.79(7), Cl(1)–Os–Cl(2) = 87.18(7), C(1)–Os–Cl(1) = 88.3(2), C(1)–Os–Cl(2) = 173.9(2), P(1)–Os–C(1) = 88.6(2), P(2)–Os–C(1) = 99.2(2).

to Cl(1). The mutual *cis* disposition of the chloride ligands indicates that the formation of this compound takes place under thermodynamic control conditions.^{18b}

The Os–C(1) distance of 2.055(8) Å compares well with the Os–C bond lengths in [Os(C₆H₄C(O)Ph)(η²-H₂){κ-C-[HNC₅H₃Et]}P(Pr₃)₂]BF₄ (2.110(5) Å) and [OsH(CH₃CN)₂{κ-C-[HNC₅H₃Et]}P(Pr₃)₂]BF₄ (1.993(6) Å),¹⁷ the tautomerized quinoline derivatives OsCl₂(η²-H₂){κ-C-[HNC₁₀H₈]}P(Pr₃)₂ (2.005(6) Å)^{9a} and OsCl₂(η²-H₂){κ-C-[HNbq]}P(Pr₃)₂ (bq = benzo[*h*]quinoline; 2.055(11) and 2.030(10) Å),^{9b} and the rare Os-imidazolynilidene complexes characterized by X-ray diffraction analysis (1.993(9)–2.123(9) Å).¹⁹

The heterocycle lies in the plane determined by the metal and the chloride ligands with the NH-hydrogen toward Cl(1). The separation between them, 2.14(11) Å, is shorter than the sum of the van der Waals radii of hydrogen and chloride (rvdw(H) = 1.20 Å, rvdw(Cl) = 1.75 Å),²⁰ suggesting that there is an intramolecular Cl···H–N hydrogen bond between these atoms,²¹ which contributes to the stabilization of the tautomer, as has been previously shown for the quinoline, 8-methylquinoline, benzo[*h*]quinoline,⁹ and 2-ethylpyridine¹⁷ NH-tautomers. The hydrogen bond is a consequence of the electrostatic interaction between the electronegative halogen and the acidic

NH-hydrogen.²² The Cl···H–N hydrogen bond is also supported by the IR in KBr, which shows the NH stretching frequency at 3106 cm^{−1} in accordance with the values reported for the related quinoline (3106 cm^{−1}), 8-methylquinoline (3130 cm^{−1}), and benzo[*h*]quinoline (3104 cm^{−1}) derivatives and by the ¹H NMR spectrum in dichloromethane-*d*₂, where the NH resonance is observed at unusually low field,²³ 14.22 ppm.

The ¹H NMR spectrum also supports the presence of an elongated dihydrogen ligand in the complex. At room temperature, this ligand displays a triplet at −10.45 ppm with a H–P coupling constant of 10.8 Hz. A variable-temperature 400 MHz *T*₁ study of the resonance gives a *T*_{1(min)} value of 40 ± 1 ms, which corresponds to a hydrogen–hydrogen distance of 1.25 Å (slow spinning).²⁴ This value, which lies in the middle of the reported range (1.0–1.5 Å) for elongated dihydrogen derivatives,²⁵ agrees well with the H–D coupling constant of 12.0 Hz obtained from the species containing the partially deuterated ligand η²-HD.²⁶

The ³¹P{¹H} NMR spectrum of **2** is consistent with the structure shown in Figure 1. As expected for two equivalent phosphine ligands, a singlet at 2.0 ppm is observed. In the ¹³C{¹H} NMR spectrum, the most noticeable resonance is a triplet (*J*_{C–P} = 7 Hz) at 182.6 ppm corresponding to C(1).

Ruthenium also promotes the tautomerization of 2-methylpyridine and stabilizes the NH-tautomer. Treatment at room temperature of dichloromethane solutions of RuH₂Cl₂(P(Pr₃)₂)₂ (**1a**) with 4.0 equiv of the heterocycle for 10 h leads to RuCl₂(η²-H₂){κ-C-[HNC₅H₃Me]}P(Pr₃)₂ (**3**), which is isolated as a yellow solid in 80% yield, according to Scheme 1.

A Cl···H–N hydrogen bond in **3** also appears to play an important role in the stabilization of the NH-tautomer. It is evident in the IR and ¹H NMR spectrum, which show the NH-stretching frequency and the NH-resonance at 3096 cm^{−1} and 14.10 ppm, respectively. In agreement with the presence of the dihydrogen ligand, the ¹H NMR spectrum in the high-field region contains at −12.76 ppm a triplet with a H–P coupling constant of 9.3 Hz. In this case, a *T*_{1(min)} value of 19 ± 1 ms in the 300 MHz scale and a H–D coupling constant of 26.4 Hz were found, which are consistent with a hydrogen–hydrogen separation of 0.98 Å. In accordance with the tautomerization of the heterocycle, the ¹³C{¹H} NMR spectrum shows at 208.0 ppm a triplet with a C–P coupling constant of 10.5 Hz, due to the metalated carbon atom. The ³¹P{¹H} NMR spectrum contains a singlet at 31.7 ppm.

(19) (a) Castarlenas, R.; Esteruelas, M. A.; Oñate, E. *Organometallics* **2005**, *24*, 4343. (b) Castarlenas, R.; Esteruelas, M. A.; Oñate, E. *Organometallics* **2007**, *26*, 2129. (c) Castarlenas, R.; Esteruelas, M. A.; Oñate, E. *Organometallics* **2007**, *26*, 3082. (d) Baya, M.; Eguillor, B.; Esteruelas, M. A.; Oliván, M.; Oñate, E. *Organometallics* **2007**, *26*, 6556. (e) Eguillor, B.; Esteruelas, M. A.; Oliván, M.; Puerta, M. *Organometallics* **2008**, *27*, 445. (f) Castarlenas, R.; Esteruelas, M. A.; Lalrempuia, R.; Oliván, M.; Oñate, E. *Organometallics* **2008**, *27*, 795.

(20) Barrio, P.; Esteruelas, M. A.; Lledós, A.; Oñate, E.; Tomás, J. *Organometallics* **2004**, *23*, 3008.

(21) (a) Castarlenas, R.; Esteruelas, M. A.; Oñate, E. *Organometallics* **2000**, *19*, 5454. (b) Castarlenas, R.; Esteruelas, M. A.; Gutiérrez-Puebla, E.; Oñate, E. *Organometallics* **2001**, *20*, 1545. (c) Buil, M. L.; Esteruelas, M. A.; Goni, E.; Oliván, M.; Oñate, E. *Organometallics* **2006**, *25*, 3076.

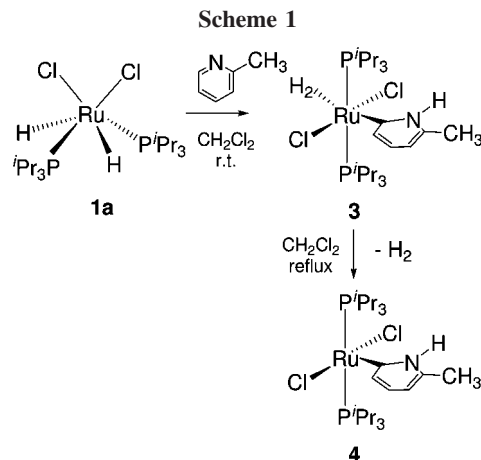
(22) (a) Stevens, R. C.; Bau, R.; Milstein, D.; Blum, O.; Koetzle, T. F. *J. Chem. Soc., Dalton, Trans.* **1990**, 1429. (b) Buil, M. L.; Esteruelas, M. A.; Oñate, E.; Ruiz, N. *Organometallics* **1998**, *17*, 3346. (c) Crochet, P.; Esteruelas, M. A.; Gutiérrez-Puebla, E. *Organometallics* **1998**, *17*, 3141. (d) Gusev, D. G.; Lough, A. J.; Morris, R. H. *J. Am. Chem. Soc.* **1998**, *120*, 13138. (e) Crabtree, R. H. *J. Organomet. Chem.* **1998**, *557*, 111. (f) Esteruelas, M. A.; Oliván, M.; Oñate, E.; Ruiz, N.; Tajada, M. A. *Organometallics* **1999**, *18*, 2953. (g) Lee, D.-H.; Kwon, H. J.; Patel, B. P.; Liabe-Sands, L. M.; Rheingold, A. L.; Crabtree, R. H. *Organometallics* **1999**, *18*, 1615. (h) Esteruelas, M. A.; Gutiérrez-Puebla, E.; López, A. M.; Oñate, E.; Tolosa, J. I. *Organometallics* **2000**, *19*, 275. (i) Barrio, P.; Esteruelas, M. A.; Oñate, E. *Organometallics* **2002**, *21*, 2491.

(23) Esteruelas, M. A.; Lahoz, F. J.; López, A. M.; Oñate, E.; Oro, L. A.; Ruiz, N.; Sola, E.; Tolosa, J. I. *Inorg. Chem.* **1996**, *35*, 7811.

(24) (a) Earl, K. A.; Jia, G.; Maltby, P. A.; Morris, R. H. *J. Am. Chem. Soc.* **1991**, *113*, 3027. (b) Desrosiers, P. J.; Cai, L.; Lin, Z.; Richards, R.; Halpern, J. *J. Am. Chem. Soc.* **1991**, *113*, 4173. (c) Jessop, P. G.; Morris, R. H. *Coord. Chem. Rev.* **1992**, *121*, 155.

(25) (a) Kubas, G. J. *Metal Dihydrogen and σ-Bond Complexes*; Kluwer Academic/Plenum Publishers: New York, 2001. (b) Heinekey, D. M.; Lledós, A.; Lluch, J. M. *Chem. Soc. Rev.* **2004**, *33*, 175. (c) Kubas, G. J. *Chem. Rev.* **2007**, *107*, 4152.

(26) Maltby, P. A.; Schlaf, M.; Steinbeck, M.; Lough, A. J.; Morris, R. H.; Klooster, W. T.; Koetzle, T. F.; Srivastava, R. C. *J. Am. Chem. Soc.* **1996**, *118*, 5396.



Complex **3**, with the chloride ligands mutually *trans* disposed, is the expected product from a kinetic control of the reaction.^{18b} When we tried to force the isomerization, to form the counterpart isomer to **2**, by heating of dichloromethane solutions of **3** at reflux temperature, the release of the coordinated hydrogen molecule and the formation of the five-coordinate complex $\text{RuCl}_2\{\kappa\text{-C}[\text{HNC}_5\text{H}_3\text{Me}]\}(\text{P}^i\text{Pr}_3)_2$ (**4**) were observed. In this context, it should be noted that ruthenium is a poorer π -back-bonder than osmium because the osmium valence orbitals have better overlap with the ligand orbitals. Thus, the $\text{Ru}(\eta^2\text{-H}_2)$ bond is weaker than the $\text{Os}(\eta^2\text{-H}_2)$ one.²⁷

Complex **4** is isolated as a green solid in 70% yield. Its ^1H , $^{13}\text{C}\{^1\text{H}\}$, and $^{31}\text{P}\{^1\text{H}\}$ NMR spectra are in agreement with those of the related 8-methylquinoline derivative, which has been characterized by X-ray diffraction analysis.^{9a} In the ^1H NMR spectrum the most noticeable signal is that corresponding to the NH-hydrogen atom, which in accordance with a $\text{Cl}\cdots\text{H}-\text{N}$ interaction is observed at 12.45 ppm. The $\text{Cl}\cdots\text{H}-\text{N}$ hydrogen bond is also supported by the IR, which shows the $\nu(\text{N}-\text{H})$ bond at 3161 cm^{-1} . In the $^{13}\text{C}\{^1\text{H}\}$ NMR spectrum, the resonance corresponding to the coordinated carbon atom of the heterocycle appears at 206.9 ppm as a triplet with a C–P coupling constant of 11 Hz. A singlet at 34.9 ppm in the $^{31}\text{P}\{^1\text{H}\}$ NMR spectrum is also characteristic of this compound.

2. Importance of the Methyl Substituent in the Tautomerization of 2-Methylpyridine. The presence of a substituent at the 2-position is required for the tautomerization of the heterocycle. In its absence, the 1,2-hydrogen shift does not occur. Under the same conditions as those used to form **2** and **3**, the treatment of **1** and **1a** with pyridine gives rise to the complexes $\text{MCl}_2\{\kappa\text{-N}[\text{NC}_5\text{H}_5]\}_3(\text{P}^i\text{Pr}_3)$ ($\text{M} = \text{Os}$ (**5**), Ru (**5a**)), containing three pyridine ligands coordinated in the usual manner, through the lone pair of the nitrogen atom instead of an *ortho*-carbon atom. The substitution of one of the phosphine ligands of **1** by pyridine is notable. In general, the *trans*- $\text{Os}(\text{P}^i\text{Pr}_3)_2$ skeleton is very stable.²⁸ Thus, previously, the displacement of one of them had been observed with polydentate

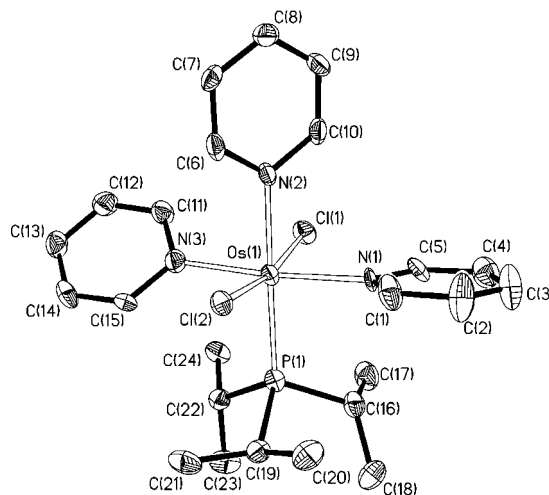
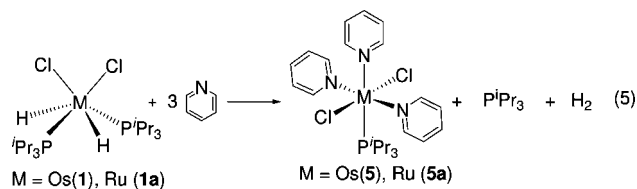


Figure 2. Molecular diagram of complex **5**. Selected bond lengths (Å) and angles (deg): $\text{Os}(1)-\text{Cl}(1) = 2.4207(19)$, $2.4293(18)$; $\text{Os}(1)-\text{Cl}(2) = 2.4214(18)$, $2.4266(18)$; $\text{Os}(1)-\text{P}(1) = 2.324(2)$, $2.342(2)$; $\text{Os}(1)-\text{N}(1) = 2.135(6)$, $2.092(6)$; $\text{Os}(1)-\text{N}(2) = 2.136(6)$, $2.127(6)$; $\text{Os}(1)-\text{N}(3) = 2.101(6)$, $2.111(6)$; $\text{Cl}(1)-\text{Os}(1)-\text{Cl}(2) = 169.77(7)$, $169.19(7)$; $\text{N}(1)-\text{Os}(1)-\text{N}(3) = 174.5(2)$, $173.5(2)$; $\text{P}(1)-\text{Os}(1)-\text{N}(2) = 178.23(17)$, $177.82(17)$.

anionic ligands.^{27b,29} Complexes **5** and **5a** are obtained as violet and yellow solids in 75% and 70% yield, respectively, according to eq 5.



The osmium complex **5** has been characterized by X-ray diffraction analysis. The structure has two chemically equivalent but crystallographically independent molecules in the asymmetric unit. A drawing of one of them is shown in Figure 2.

The coordination geometry around the osmium atom can be rationalized as a distorted octahedron with *mer* pyridine groups ($\text{N}(1)-\text{Os}(1)-\text{N}(3) = 174.5(2)^\circ$ and $173.5(7)^\circ$), *trans* chloride ligands ($\text{Cl}(1)-\text{Os}(1)-\text{Cl}(2) = 169.77(7)^\circ$ and $169.19(7)^\circ$), and the phosphine *trans* disposed to $\text{N}(2)$ ($\text{P}(1)-\text{Os}(1)-\text{N}(2) = 178.23(17)^\circ$ and $177.82(17)^\circ$). In agreement with the presence of the phosphine ligand, the $^{31}\text{P}\{^1\text{H}\}$ NMR spectra of **5** and **5a** show singlets at -20.4 and 37.9 ppm, respectively.

The formation of **5** and **5a** according to eq 5 suggests that the steric hindrance experienced between the heterocycle, in particular the 2-substituent, and the ligands of the metal precursor is determinant for the tautomerization. In agreement with this we have also observed that, in contrast to benzophenone, methyl vinyl ketone releases 2-ethylpyridine from $[\text{OsH}(\eta^2\text{-CH}_2=\text{CH}-o\text{-C}_5\text{H}_4\text{N})(\eta^2\text{-H}_2)(\text{P}^i\text{Pr}_3)_2]\text{BF}_4$.¹⁷ These results are consistent with the observations of Carmona's group.

In contrast to 2-substituted pyridines, the unsubstituted substrate reacts with $\text{Tp}^{\text{Me}_2}\text{IrPh}_2(\text{N}_2)$ to yield a very stable N-coordinated adduct.^{8a} However, the reaction of the more congested precursor $\text{Tp}^{\text{Ms}}\text{Ir}(\text{N}_2)$ (Ms = metalated mesityl substituents) affords a 1:1 kinetic mixture of species containing the usual tautomer and NH-tautomer of the pyridine.^{8b}

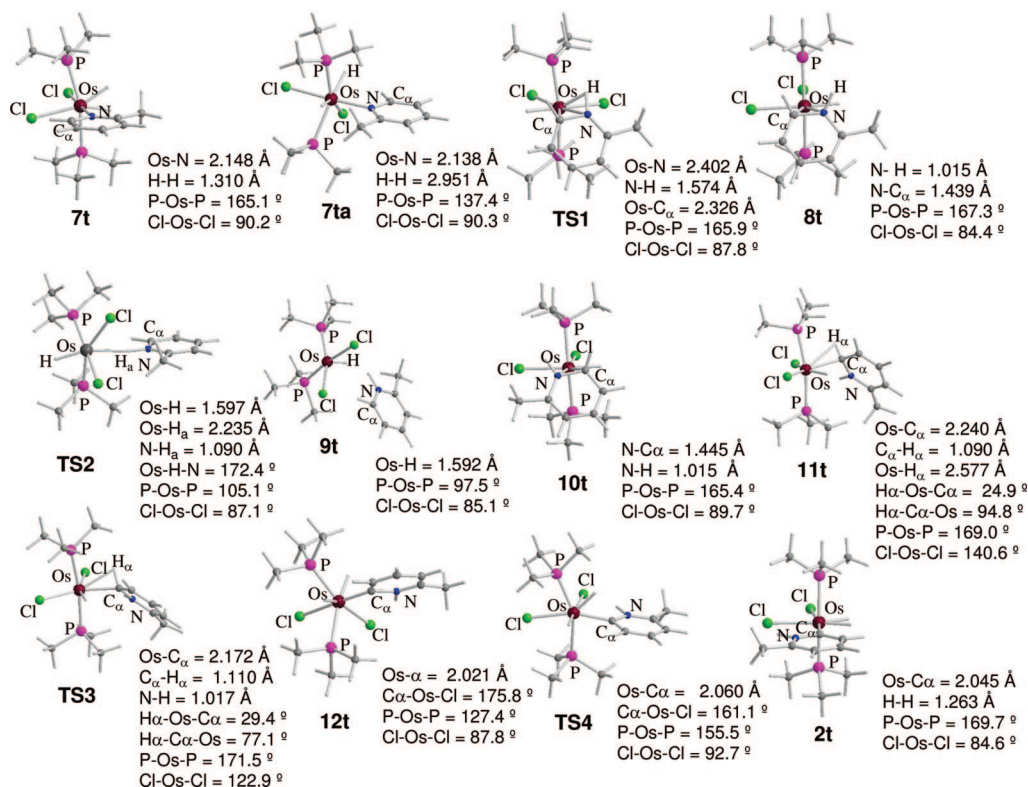
3. Theoretical Calculations on the Tautomerization Process. At 100°C , the treatment of toluene- d_8 solutions of the dideuteride complex $\text{OsD}_2\text{Cl}_2(\text{P}^i\text{Pr}_3)_2$ (**1-d₂**) with excess of

(27) (a) Bautista, M. T.; Cappellani, E. P.; Drouin, S. D.; Morris, R. H.; Schweitzer, C. T.; Sella, A.; Zubkowski, J. *J. Am. Chem. Soc.* **1991**, *113*, 4876. (b) Bohanna, C.; Esteruelas, M. A.; Gómez, A. V.; López, A. M.; Martínez, M.-P. *Organometallics* **1997**, *16*, 4464.

(28) Esteruelas, M. A.; Oro, L. A. *Adv. Organomet. Chem.* **2001**, *47*, 1.

(29) (a) Esteruelas, M. A.; Gómez, A. V.; López, A. M.; Oro, L. A. *Organometallics* **1996**, *15*, 878. (b) Esteruelas, M. A.; López, A. M.; Ruiz, N.; Tolosa, J. I. *Organometallics* **1997**, *16*, 4657. (c) Esteruelas, M. A.; López, A. M.; Oñate, E.; Royo, E. *Organometallics* **2004**, *23*, 3021. (d) Esteruelas, M. A.; López, A. M.; Oñate, E.; Royo, E. *Organometallics* **2004**, *23*, 5633. (e) Esteruelas, M. A.; López, A. M.; Oñate, E.; Royo, E. *Organometallics* **2005**, *24*, 5780. (f) Castro-Rodrigo, R.; Esteruelas, M. A.; López, A. M.; Oliván, M.; Oñate, E. *Organometallics* **2007**, *26*, 4498.

Chart 1



2-methylpyridine and quinoline leads after 48 h to **2** and the related quinoline complex $\text{OsCl}_2(\eta^2\text{-H}_2)\{\kappa\text{-C-[HNC}_9\text{H}_6]\}(\text{P}^i\text{Pr}_3)_2$ (**6**),^{9a} respectively, which do not contain significant amounts of deuterium. The presence of hydrogen at the metal center of **2** and **6** proves that, as expected, the tautomerization occurs through the metal center, whereas the absence of detectable amounts of deuterium in the obtained complexes indicates that the processes are reversible. In agreement with the latter we have also observed that the quinoline of **6** is displaced by perdeuterated quinoline.

In an effort to gain insight into the mechanistic details of these interesting processes we have carried out DFT calculations (B3PW91) on the tautomerization of 2-methylpyridine and quinoline promoted by **1** using PMe_3 as a model of P^iPr_3 . The changes in free energy (ΔG) have been computed at 298.15 K and $P = 1$ atm.

The addition of the usual tautomer of 2-methylpyridine to $\text{OsH}_2\text{Cl}_2(\text{PMe}_3)_2$ (**1t**) is an exoergic process. The coordination via the lone pair of the nitrogen atom is favored with regard to the coordination through the C-N³⁰ and C-C bonds. It affords an elongated dihydrogen species $\text{OsCl}_2(\eta^2\text{-H}_2)\{\kappa\text{-N-[NC}_5\text{H}_4\text{Me]}\}(\text{PMe}_3)_2$ (**7t** in Chart 1), which is 3.2 kcal·mol⁻¹ more stable than the **1t** plus 2-methylpyridine pair. This octahedral compound has *trans*-phosphines (P-Os-P = 165.1°) and *cis*-chloride (Cl-Os-Cl = 90.2°) ligands. The dihydrogen molecule is almost parallel to the P-Os-P direction. The hydrogen atoms are separated by 1.310 Å.

Complex **7t** is an 18-valence electron species. Due to its saturated character, it cannot promote the activation of the C α -H α bond of the heterocycle. However, it could evolve by hydrogen shift from the metal center to the nitrogen atom or alternatively by dissociation of some ligand.

The hydrogen transfer from the metal to the nitrogen atom requires, as a previous stage, the position exchange between a phosphine and a hydrogen atom of the dihydrogen molecule. The resulting dihydride **7ta** is 11.3 kcal·mol⁻¹ less stable than **7t**. The subsequent osmium to nitrogen hydrogen migration leads to a $\eta^2\text{-C-N}$ -pyridinium species **8t**, which lies 25.7 kcal·mol⁻¹ above the **1t** plus 2-methylpyridine pair. The transition state **TS1** connecting **7ta** and **8t** results from the concerted approaches of the hydride ligand of **7ta**, disposed *transoid* to one of the phosphines (P-Os-H = 156.3°) to the nitrogen, and the C α -carbon atom of the heterocycle to the metal center. It is 48.9 kcal·mol⁻¹ above **7t**. So, the energy for the hydrogen shift is too large for the experimental conditions used in the tautomerization. The necessary energies for the migrations starting from the $\eta^2\text{-C,C}$ isomers of **7t** are even larger (see Supporting Information).

The dissociation of some ligand is not feasible from a real point of view. The dissociation of one of the triisopropylphosphine ligands should prevent the tautomerization, since the steric hindrance between the substituent of the heterocycle and the phosphines, determinant for the process, should undergo a significant reduction. Due to the preference of osmium for coordination saturation³¹ and the polarity of the used solvent in the reaction, toluene, the dissociation of chloride does not appear to be reasonable. Furthermore, the computed activation energy for the tautomerization via an ionic mechanism is higher than 33.4 kcal·mol⁻¹ (see Supporting Information) and higher than that found for an intermolecular osmium to nitrogen hydrogen migration (*vide infra*).

(30) Any minimum containing a coordinated $\eta^2\text{-C,N}$ ligand has not been found.

(31) See for example: (a) Bolaño, T.; Castarlenas, R.; Esteruelas, M. A.; Modrego, F. J.; Oñate, E. *J. Am. Chem. Soc.* **2005**, *127*, 11184. (b) Bolaño, T.; Castarlenas, R.; Esteruelas, M. A.; Oñate, E. *J. Am. Chem. Soc.* **2006**, *128*, 3965. (c) Bolaño, T.; Castarlenas, R.; Esteruelas, M. A.; Oñate, E. *Organometallics* **2007**, *26*, 2037. (d) Bolaño, T.; Castarlenas, R.; Esteruelas, M. A.; Oñate, E. *J. Am. Chem. Soc.* **2007**, *129*, 8850.

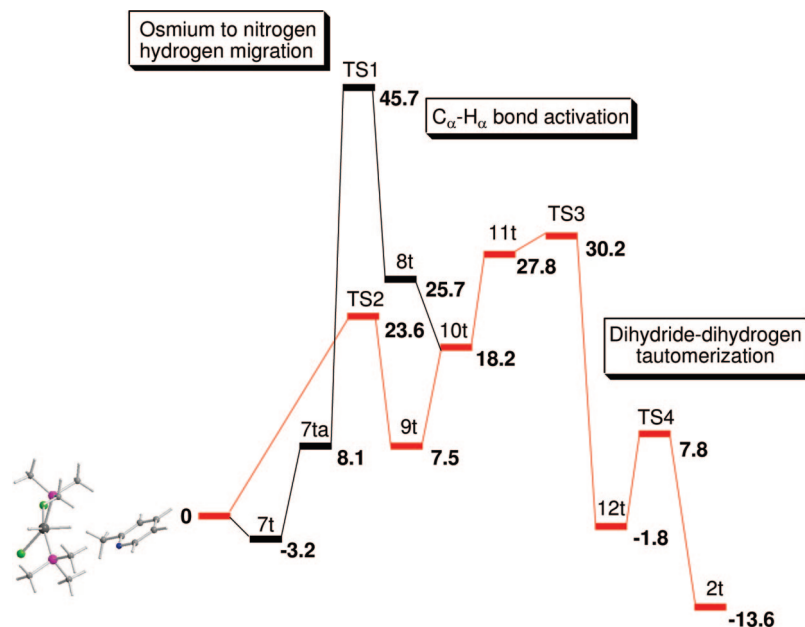


Figure 3. Energy profile (ΔG in $\text{kcal} \cdot \text{mol}^{-1}$) for the NH-tautomerization of 2-methylpyridine on $\text{OsH}_2\text{Cl}_2(\text{PMe}_3)_2$. Black: via intramolecular osmium to nitrogen hydrogen migration. Red: via intermolecular osmium to nitrogen hydrogen migration.

Figure 3 shows the energy profile for the mechanism including an intermolecular hydrogen transfer from the metal center to the nitrogen atom of the heterocycle, whereas Chart 1 collects the optimized structures and selected structural parameters. The intermolecular osmium to nitrogen hydrogen migration leads to the $[\text{HNC}_5\text{H}_4\text{Me}]^+[\text{OsHCl}_2(\text{PMe}_3)_2]^-$ (**9t**) cation–anion pair, which is $7.5 \text{ kcal} \cdot \text{mol}^{-1}$ less stable than the **1t** plus 2-methylpyridine pair. The anion can be described as a square-pyramidal species with the hydride in the apical position and *cis*-phosphines ($\text{P}-\text{Os}-\text{P} = 97.5^\circ$) and *cis*-chlorides ($\text{Cl}-\text{Os}-\text{Cl} = 85.1^\circ$) in the base. The hydrogen abstraction takes place via the **TS2** transition state, which lies $23.6 \text{ kcal} \cdot \text{mol}^{-1}$ above the **1t** plus 2-methylpyridine pair and $22.1 \text{ kcal} \cdot \text{mol}^{-1}$ below the transition state for the intramolecular migration (**TS1**). It is a pseudo-octahedral species, where one of the hydride ligands of **1t** is separated by 2.234 \AA from the osmium atom by action of the lone pair of the nitrogen atom of the heterocycle.

Once the metal to nitrogen hydrogen migration has taken place, the $\text{C}_\alpha-\text{H}_\alpha$ bond activation of the resulting 2-methylpyridinium occurs. This second process is initiated by the coordination of the $\text{C}-\text{N}$ bond of the protonated heterocycle to the metal center of $[\text{OsHCl}_2(\text{PMe}_3)_2]^-$. The resulting $\eta^2\text{-C}_\alpha\text{N}$ -pyridinium intermediate **10t** is an isomer of **8t**. Complex **10t** is $7.5 \text{ kcal} \cdot \text{mol}^{-1}$ more stable than the latter. In contrast to **8t**, the NH-hydrogen atom of the coordinated heterocycle of **10t** is *cisoid* disposed with regard to one of the chloride ligands. The separation between them, 3.084 \AA , is similar to the sum of the van der Waals radii of hydrogen and chloride and slightly shorter than the separation between the related chloride and the CH-hydrogen atom in **8t** (3.151 \AA). This suggests that a weak intramolecular $\text{Cl} \cdots \text{H}-\text{N}$ hydrogen bond contributes to the stabilization of **10t** with regard to **8t**. Like the latter, intermediate **10t** is an octahedral species with *trans*-phosphines ($\text{P}-\text{Os}-\text{P} = 165.4^\circ$) and *cis*-chlorides ($\text{Cl}-\text{Os}-\text{Cl} = 89.7^\circ$). Complex **10t** closes the $\text{Cl} \cdots \text{H}-\text{N}$ hydrogen bond to afford **11t**, where the separation between the chloride and the NH-hydrogen atom is 2.688 \AA . Their approach provokes the slippage of the metal center from the $\text{C}_\alpha-\text{N}$ bond to the $\text{C}_\alpha-\text{H}_\alpha$ one. The bond lengths within the $\text{H}_\alpha\text{C}_\alpha\text{Os}$ unit are 2.244 ($\text{Os}-\text{C}_\alpha$), 1.090 ($\text{C}_\alpha-\text{H}_\alpha$), and 2.577 ($\text{Os}-\text{H}_\alpha$) \AA . Intermediate **11t** is $9.6 \text{ kcal} \cdot \text{mol}^{-1}$ less

stable than **10t**. The rupture of the $\text{C}_\alpha-\text{H}_\alpha$ bond takes place through **TS3** and gives rise to the dihydride **12t**. As expected, in **TS3**, the $\text{C}_\alpha-\text{H}_\alpha$ (1.111 \AA) bond is extended while $\text{Os}-\text{H}_\alpha$ (2.207 \AA) and $\text{Os}-\text{C}_\alpha$ (2.172 \AA) separations are shortened. Also, the $\text{Cl} \cdots \text{H}-\text{N}$ (2.560 \AA) hydrogen bond is slightly intensified. The transition state **TS3** lies $6.6 \text{ kcal} \cdot \text{mol}^{-1}$ above **TS2** and $15.5 \text{ kcal} \cdot \text{mol}^{-1}$ below **TS1**. It is the crest of the overall process. Thus, the $\text{C}_\alpha-\text{H}_\alpha$ bond activation is the rate-determining step of the tautomerization process of 2-methylpyridine.

The final product **2t** results from a dihydride–dihydrogen tautomerization at **12t**, via the transition state **TS4**. Intermediate **12t** is a seven-coordinate species. Its structure can be described as a pentagonal bipyramid with the heterocycle and one of the chloride ligands in apical positions ($\text{Cl}-\text{Os}-\text{C}_\alpha = 175.8^\circ$). The hydride ligands lie in the base, one of them between the phosphines and the other one between a phosphine and a chloride. This complex is $1.8 \text{ kcal} \cdot \text{mol}^{-1}$ more stable than the **1t** plus 2-methylpyridine pair and $11.8 \text{ kcal} \cdot \text{mol}^{-1}$ less stable than the elongated dihydrogen **2t**. During the tautomerization, the hydride ligand situated between a phosphine and a chloride leaves the base of the pyramid and approaches the other one. In **TS4** the hydrogen–hydrogen separation is 2.304 \AA . Along the process the $\text{Cl} \cdots \text{H}-\text{N}$ hydrogen bond is intensified. Thus, the $\text{Cl}-\text{H}$ distance is shortened from 2.115 \AA in **12t** to 2.020 \AA in **TS4**. The barrier for the dihydride–dihydrogen tautomerization is $9.6 \text{ kcal} \cdot \text{mol}^{-1}$.

The formation of **2** is a process of three stages, according to the results previously mentioned. They are (i) an intermolecular osmium to nitrogen hydrogen migration, (ii) the $\text{C}_\alpha-\text{H}_\alpha$ bond activation of the resulting protonated heterocycle to afford a dihydride species, and (iii) the dihydride–dihydrogen tautomerization of the dihydride. The rate-determining stage is the $\text{C}_\alpha-\text{H}_\alpha$ bond activation. The tautomerization of quinoline to give **6** is a similar process. The same intermediates and transition states with quinoline instead of 2-methylpyridine have been found. Figure 4 shows its energy profile, whereas Chart 2 collects the optimized structures and selected structural parameters.

The intermolecular osmium to nitrogen hydrogen migration does not show any difference between quinoline and 2-methylpyridine. For quinoline, the activation barrier of this stage is

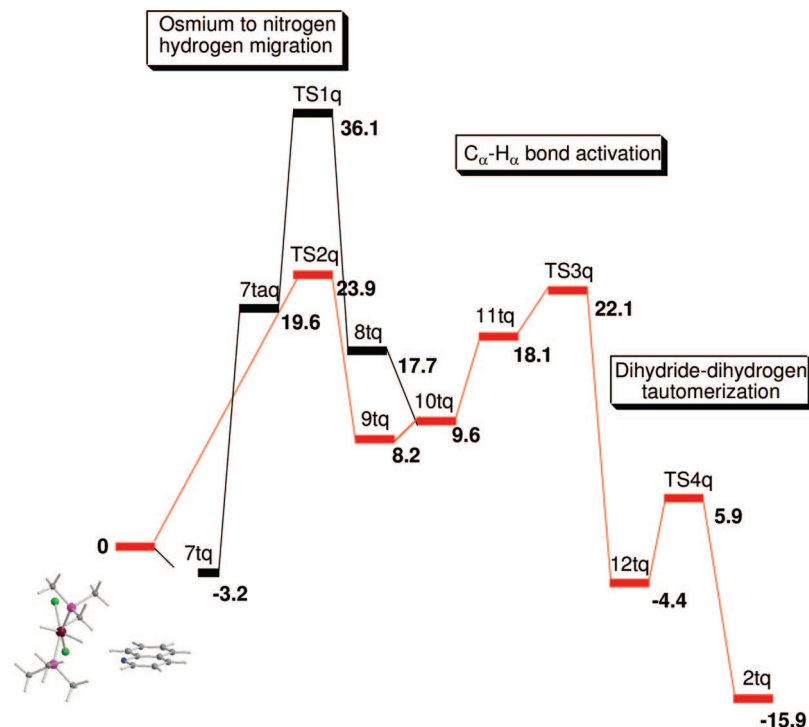
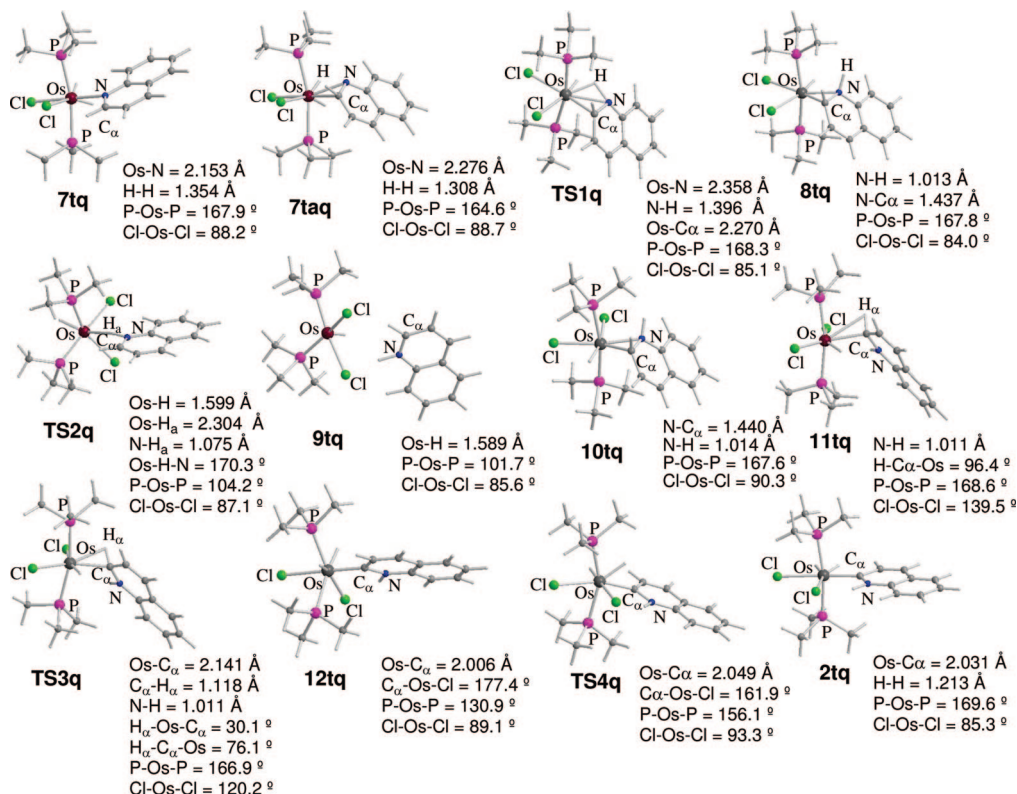


Figure 4. Energy profile (ΔG in $\text{kcal} \cdot \text{mol}^{-1}$) for the NH-tautomerization of quinoline on $\text{OsH}_2\text{Cl}_2(\text{PMe}_3)_2$. Black: via intramolecular osmium to nitrogen hydrogen migration. Red: via intermolecular osmium to nitrogen hydrogen migration.

Chart 2



$23.9 \text{ kcal} \cdot \text{mol}^{-1}$, i.e., $0.3 \text{ kcal} \cdot \text{mol}^{-1}$ higher than for 2-methylpyridine. The energy cost for the last stage, the dihydride-dihydrogen tautomerization, is also very similar for both heterocycles. The energy barrier for the **12tq** tautomerization, $10.3 \text{ kcal} \cdot \text{mol}^{-1}$, is only $0.7 \text{ kcal} \cdot \text{mol}^{-1}$ higher than that for the 2-methylpyridine case. However, the $\text{C}\alpha\text{-H}\alpha$ bond activation is favored for quinoline. The reason appears to be the capacity

of its fused carbocycle to delocalize electron density of the metal center, which stabilizes the intermediates **10tq** and **11tq**. Thus, while the energy difference between the $\eta^2\text{-C,N}$ -protonated heterocycle intermediates **10tq** and **10t** and the corresponding transition states **TS3q** and **TS3** is about $12 \text{ kcal} \cdot \text{mol}^{-1}$ in both cases, the coordination of the protonated heterocycle to the metal center of $[\text{OsHCl}_2(\text{PMe}_3)_2]^-$ is less endoergic by $9.3 \text{ kcal} \cdot \text{mol}^{-1}$

for quinoline than for 2-methylpyridine. As a result, **TS3q** lies 1.8 kcal·mol⁻¹ below **TS2q**, and therefore the intermolecular osmium to nitrogen hydrogen migration is converted into the rate-determining stage for the quinoline tautomerization.

In light of these results, the role of the Cl···H–N hydrogen bond and the hydride nature of **1** should be pointed out. The Cl···H–N hydrogen bond determines not only the stability of the metal complex containing the NH-tautomer of the heterocycle but also the course of the tautomerization process. Although several mechanisms are possible, that initiated with an intermolecular metal to nitrogen hydrogen migration has the lowest activation energy. According to this, transition-metal hydride complexes should favor the NH-tautomerization of 2-substituted nitrogen containing heterocycles. In this context, the p*K*_a of the complex is a main factor, which should be taken into account in order to choose the hydride promotor.

Concluding Remarks

This study has revealed that complexes MH₂Cl₂(PⁱPr₃)₂ (M = Ru, Os) promote the NH-tautomerization and stabilize the resulting NH-tautomers not only of quinolines but also of 2-substituted pyridines. The steric demand of the heterocycles is determinant for the tautomerization. An intramolecular Cl···H–N hydrogen bond between a chloride ligand and the NH-hydrogen of the tautomerized heterocycle plays a main role in the stabilization and in the formation of the isolated dihydrogen complexes, containing the heterocycle coordinated by the C_α atom. DFT calculations indicate that these compounds are formed in three stages, including an intermolecular metal to nitrogen hydrogen migration, the subsequent C_α–H bond activation of the protonated heterocycle, and finally the dihydride–dihydrogen tautomerization of the resulting dihydride. The rate-determining step depends on the heterocycle.

In conclusion, we have achieved an understanding and a rationalization of the NH-tautomerization of 2-substituted pyridines and quinolines promoted by MH₂Cl₂(PⁱPr₃)₂ (M = Ru, Os).

Experimental Section

General Information. All manipulations were performed with rigorous exclusion of air at an argon/vacuum manifold using standard Schlenk-tube techniques or in a drybox (MB-UNILAB). Solvents were dried by the usual procedures and distilled under argon prior to use. 2-Methylpyridine and pyridine (Aldrich) were used without further purification. The starting materials MH₂Cl₂(PⁱPr₃)₂ (M = Os (**1**),³² Ru (**1a**)³³) and OsD₂Cl₂(PⁱPr₃)₂ (**1-d**)^{9b} were prepared in accordance with methods reported in the literature.

NMR spectra were recorded on either a Varian Gemini 2000, a Bruker ARX 300, a Bruker Avance 300 MHz, or a Bruker Avance 400 MHz instrument. Chemical shifts (expressed in parts per million) are referenced to residual solvent peaks (¹H, ¹³C{¹H}) or external H₃PO₄ (³¹P{¹H}). Coupling constants, *J*, are given in hertz. The *d*_{H–H} were calculated based on published methods^{24a,26} using both the *T*_{1min} and *J*_{HD} experimental values. Infrared spectra were recorded on a Perkin-Elmer Spectrum One FT-IR spectrometer. C, H, and N analyses were carried out in a Perkin-Elmer 2400 CHNS/O analyzer.

(32) Aracama, M.; Esteruelas, M. A.; Lahoz, F. J.; Lopez, J. A.; Meyer, U.; Oro, L. A.; Werner, H. *Inorg. Chem.* **1991**, *30*, 288.

(33) (a) Grünwald, C.; Gevert, O.; Wolf, J.; González-Herrero, P.; Werner, H. *Organometallics* **1996**, *15*, 1960. (b) Oliván, M.; Clot, E.; Eisenstein, O.; Caulton, K. G. *Organometallics* **1998**, *17*, 3091.

Preparation of OsCl₂(η²-H₂){κ-C-[HNC₅H₃Me]}(PⁱPr₃)₂ (**2**).

A Young's tap Schlenk was charged with **1** (200 mg, 0.343 mmol), 2-methylpyridine (0.27 mL, 2.72 mmol), and toluene (15 mL). The mixture was heated at 95 °C for 48 h. The dark solution was filtered through Celite, and the solvent was removed *in vacuo*. The residue was washed with pentane (10 mL). The orange residue was recrystallized from acetone to give a yellow solid. Yield: 150 mg (65%). Anal. Calcd for C₂₄H₅₁Cl₂NOsP₂: C, 42.59; H, 7.59; N, 2.07. Found: C, 42.54; H, 7.99; N, 2.02. ¹H NMR (300 MHz, CD₂Cl₂, 293 K): δ 14.22 (br, 1H, NH), 7.52 (m, 1H), 6.92 (m, 1H), 6.46 (m, 1H), 2.33 (s, 3H, CH₃-py), 2.28 (m, 6H, CH-ⁱPr), 1.19 (dvt, 18H, *J*_{H–H} = 6.9, *N* = 12.6, CH₃-ⁱPr), 1.17 (dvt, 18H, *J*_{H–H} = 6.6, *N* = 12.3, CH₃-ⁱPr), –10.45 (t, 2H, *J*_{P–H} = 10.8 Hz, OsH₂). ¹³C{¹H} NMR (75.45 MHz, CD₂Cl₂, 293 K, plus APT): δ 182.6 (t, *J*_{P–C} = 7, 1C, Os–C), 147.9 (s, 1C, C_{ipso}), 146.8 (s, 1C, CH), 135.1 (s, 1C, CH), 114.0 (s, 1C, CH), 25.3 (t, *J*_{P–C} = 12, 6C, CH-ⁱPr), 19.5 (s, 6C, CH₃-ⁱPr), 19.1 (s, 6C, CH₃-ⁱPr), 18.9 (s, 1C, CH₃-py). ³¹P{¹H} NMR (121.42 MHz, C₆D₆, 293 K): δ 2.0 (s). *T*_{1(min)} (ms, CD₂Cl₂, –10.56, 400 MHz, 228 K): 40 ± 1 ⇒ *d*_{H–H} calc = 1.25 Å. IR (KBr, cm⁻¹): 3106 ν(N–H), 2230 ν(Os–H₂).

Determination of the *J*_{H–D} Value for Complex **2.** A Young's tap NMR tube was charged with 2-methylpyridine (19 mg, 20 mmol), OsD₂Cl₂(PⁱPr₃)₂ (30 mg, 0.05 mmol), and toluene-*d*₈ (0.75 mL). The mixture was heated at 95 °C for 24 h. After that the solvent was removed *in vacuo* and CD₂Cl₂ (0.50 mL) and CD₃OD (0.05 mL) were added. The ¹H{³¹P} NMR spectra of these solutions exhibit in the hydride region the resonances due to a mixture of the [Os](η²-H–D) and the [Os](η²-H–H) **2** species. *J*_{H–D} (Hz) = 12.0 ⇒ *d*_{H–H} calc = 1.22 Å.

Preparation of RuCl₂(η²-H₂){κ-C-[HNC₅H₃Me]}(PⁱPr₃)₂ (**3**).

2-Methylpyridine (0.16 mL, 1.60 mmol) was added to a CH₂Cl₂ (5 mL) solution of **1a** (200 mg, 0.404 mmol). The mixture was stirred for 10 h. The solvent was removed *in vacuo*. The residue was washed with pentane to afford a yellowish-green solid. The solid was dissolved in CH₂Cl₂ (2 mL) and precipitated with diethyl ether (15 mL) to give a yellow solid. Yield: 190 mg (80%). Anal. Calcd for C₂₄H₅₁Cl₂NP₂Ru: C, 49.06; H, 8.75; N, 2.38. Found: C, 49.04; H, 8.90; N, 2.61. ¹H NMR (300 MHz, CD₂Cl₂, 293 K): δ 14.10 (br, 1H, NH), 7.33 (m, 1H), 6.90 (m, 1H), 6.48 (m, 1H), 2.36 (s, 3H, CH₃-py), 2.31 (m, 6H, CH-ⁱPr), 1.29 (dvt, 18H, *J*_{H–H} = 6.9, *N* = 20.4, CH₃-ⁱPr), 1.25 (dvt, 18H, *J*_{H–H} = 6.6, *N* = 20.4, CH₃-ⁱPr), –12.76 (t, 2H, *J*_{P–H} = 9.3 Hz, RuH₂). ¹³C{¹H} NMR (100 MHz, CD₂Cl₂, 293 K, plus APT): δ 208.0 (t, *J*_{P–C} = 10.5, 1C, Ru–C), 148.5 (s, 1C, C_{ipso}), 144.9 (s, 1C, CH), 133.4 (s, 1C, CH), 114.4 (s, 1C, CH), 25.1 (t, *J*_{P–C} = 9.5, 6C, CH-ⁱPr), 19.5 (s, 6C, CH₃-ⁱPr), 19.72 (s, 6C, CH₃-ⁱPr), 18.9 (s, 1C, CH₃-py). ³¹P NMR (121.42 MHz, CD₂Cl₂, 293 K): δ 31.7 (s). *T*_{1(min)} (ms, CD₂Cl₂, –12.90, 300 MHz, 228 K): 19 ± 1 ⇒ *d*_{H–H} calc = 0.92 Å. IR (KBr, cm⁻¹): 3096 ν(N–H), 1997 ν(RuH₂).

Determination of the *J*_{H–D} Value for Complex **3.** A Young's tap NMR tube was charged with **3** (0.05 mmol), CD₂Cl₂ (0.60 mL), and CD₃OD (0.15 mL). After 24 h the ¹H{³¹P} NMR spectra of this solution exhibited in the hydride region the resonances due to a mixture of the [Ru](η²-H–D) and the [Ru](η²-H–H) species. *J*_{H–D} (Hz) = 26.4 ⇒ *d*_{H–H} calc = 0.98 Å.

Preparation of RuCl₂{κ-C-[HNC₅H₃Me]}(PⁱPr₃)₂ (**4**).

A CH₂Cl₂ (15 mL) solution of **3** (150 mg, 0.256 mmol) was refluxed for 16 h. The resulting green solution was filtrated through Celite, and the solvent was removed *in vacuo*. The residue was extracted with diethyl ether. The diethyl ether solution was concentrated *in vacuo* to (≈3 mL). Addition of pentane (20 mL) caused the precipitation of a green solid, which was dried *in vacuo*. Yield: 110 mg (70%). Anal. Calcd for C₂₄H₄₉Cl₂NRuP₂: C, 49.22; H, 8.43; N, 2.39. Found: C, 49.56; H, 8.37; N, 2.61. ¹H NMR (300 MHz, CD₂Cl₂, 293 K): δ 12.45 (br, 1H, NH), 8.22 (m, 1H), 6.53 (m, 1H), 6.17 (m, 1H), 2.96 (m, 6H, CH-ⁱPr), 2.18 (3H, CH₃-py), 1.21 (dvt, 18H, *J*_{H–H} = 6.3, *N* = 18.3, CH₃-ⁱPr), 1.19 (dvt, 18H, *J*_{H–H} =

6.0, $N = 23.4$, $\text{CH}_3\text{-}^1\text{Pr}$). $^{13}\text{C}\{^1\text{H}\}$ NMR (75.45 MHz, CD_2Cl_2 , 293 K, plus APT): δ 206.9 (t, $J_{\text{P-C}} = 11$, 1C, Ru-C), 146.6 (s, 1C, C_{ipso}), 142.3 (s, 1C, CH), 127.3 (s, 1C, CH), 111.4 (s, 1C, CH), 23.2 (t, $J_{\text{P-C}} = 8$, 6C, $\text{CH-}^1\text{Pr}$), 19.9 (s, 6C, $\text{CH}_3\text{-}^1\text{Pr}$), 19.5 (s, 6C, $\text{CH}_3\text{-}^1\text{Pr}$), 18.8 (s, 1C, $\text{CH}_3\text{-py}$). $^{31}\text{P}\{^1\text{H}\}$ NMR (121.42 MHz, C_6D_6 , 293 K): δ 34.9 (s). IR (KBr, cm^{-1}): 3161 $\nu(\text{N-H})$.

Reaction of 4 with H_2 . A CD_2Cl_2 solution (0.5 mL) of **4** (50 mg, 0.0085 mmol) was prepared under an atmosphere of H_2 in a Young's tap NMR tube. After 7 h the ^1H and ^{31}P NMR spectra of these solutions showed a 7/2 mixture of complexes **3** and **4**, respectively.

Preparation of $\text{OsCl}_2\{\kappa\text{-N-}[\text{NC}_5\text{H}_5]\}_3(\text{P}^i\text{Pr}_3)$ (5**).** Pyridine (64 μL , 0.81 mmol) was added to a toluene (15 mL) solution of **1** (150 mg, 0.257 mmol). The mixture was refluxed for 10 h to give a dark red solution. The solution was filtrated through Celite, and the solvent was removed *in vacuo* to give a dark residue, which was washed with pentane (10 mL) and extracted with diethyl ether. The ether solution was filtered through Celite, concentrated to half of the volume, and stored at -20°C to afford violet crystals. Yield: 127 mg (75%). Anal. Calcd for $\text{C}_{24}\text{H}_{36}\text{Cl}_2\text{N}_3\text{OsP}$: C, 43.76; H, 5.50; N, 6.38. Found: C, 43.96; H, 5.71; N, 6.18. ^1H NMR (300 MHz, C_6D_6 , 293 K): δ 9.83 (m, 4H, py-cis), 8.51 (m, 2H, CH, py-trans), 6.73 (m, 3H, CH, py-trans), 6.34 (m, 6H, CH, py-cis), 2.80 (m, 3H, $\text{CH-}^1\text{Pr}$), 1.42 (dd, 18H, $J_{\text{H-H}} = 7.2$, $J_{\text{H-P}} = 11.7$, $\text{CH}_3\text{-}^1\text{Pr}$). $^{13}\text{C}\{^1\text{H}\}$ NMR (100 MHz, C_6D_6 , 293 K, plus APT): δ 160.0 (s, 4C, CH, py-cis), 154.3 (2C, CH, py-trans), 134.4 (s, 1C, CH, py-trans), 132.9 (s, 2C, CH, py-cis), 123.6 (s, 2C, CH, py-trans), 123.3 (s, 4C, CH, py-cis), 27.3 (d, $J_{\text{P-C}} = 22.9$, 3C, $\text{CH-}^1\text{Pr}$), 19.8 (s, 6C, $\text{CH}_3\text{-}^1\text{Pr}$), $^{31}\text{P}\{^1\text{H}\}$ NMR (121.42 MHz, C_6D_6 , 293 K): δ -20.4 (s).

Preparation of $\text{RuCl}_2\{\kappa\text{-N-}[\text{NC}_5\text{H}_5]\}_3(\text{P}^i\text{Pr}_3)$ (5a**).** Pyridine (0.10 mL, 1.20 mmol) was added to a toluene (15 mL) solution of **1a** (150 mg, 0.303 mmol). The mixture was stirred at rt for 10 h to give an orange solution. The solution was filtrated through Celite, and the solvent was removed *in vacuo* to give a yellow residue, which was washed with pentane (10 mL) and extracted with diethyl ether to give a yellow solid. Yield: 123 mg (70%). Anal. Calcd for $\text{C}_{24}\text{H}_{36}\text{Cl}_2\text{N}_3\text{PRu}$: C, 50.61; H, 6.37; N, 7.38. Found: C, 50.47; H, 6.44; N, 7.42. ^1H NMR (300 MHz, CD_2Cl_2 , 293 K): δ 9.41 (m, 4H, CH, py-cis), 8.38 (m, 2H, CH, py-trans), 7.57 (m, 3H, CH, py-trans), 7.04 (m, 6H, CH, py-cis), 2.50 (m, 3H, $\text{CH-}^1\text{Pr}$), 1.21 (dd, 18H, $J_{\text{H-H}} = 7.2$, $J_{\text{H-P}} = 11.7$, $\text{CH}_3\text{-}^1\text{Pr}$). $^{13}\text{C}\{^1\text{H}\}$ NMR (75.45 MHz, CD_2Cl_2 , 293 K): δ 158.7 (s, 4C, $J_{\text{P-C}} = 12$, CH, py-cis), 154.7 (s, 2C, CH, py-trans), 135.3 (s, 1C, CH, py-trans), 134. Five (s, 2C, CH, py-cis), 123.2 (s, 2C, CH, py-trans), 123.0 (s, 4C, CH, py-cis), 26.0 (d, $J_{\text{P-C}} = 16.8$, 3C, $\text{CH-}^1\text{Pr}$), 19.5 (s, 6C, $\text{CH}_3\text{-}^1\text{Pr}$), $^{31}\text{P}\{^1\text{H}\}$ NMR (121.42 MHz, CD_2Cl_2 , 293 K): δ 37.9 (s).

Computational Details. The calculations have been carried out using the Gaussian 03 computational package.³⁴ All the structures have been optimized using DFT and the B3PW91 functional. The 6-31G** basis set has been used for all the non-hydrogen atoms and hydride ligands, with the exception of the methyl groups of the PMe_3 ligands and the hydrogen atoms of the N-heterocycles (6-31G) and the Os atom (LANL2DZ basis and pseudopotential). The transition states found have been confirmed by frequency calculations, and the connection between the starting and final reactants has been checked by slightly perturbing the TS geometry toward the minima geometries and reoptimizing.

Structural Analysis of Complexes 2 and 5. Crystals suitable for the X-ray diffraction study were obtained by cooling at -30°C $\text{CH}_2\text{Cl}_2/\text{Et}_2\text{O}$ (**2**) or toluene (**5**) solutions. X-ray data were collected for all complexes on a Bruker Smart APEX CCD diffractometer equipped with a normal focus, 2.4 kW sealed tube source (Mo radiation, $\lambda = 0.71073$ Å) operating at 50 kV and 40 mA. Data were collected over the complete sphere by a combination of four sets. Each frame exposure time was 10 s (**2**) or 20 s (**5**) covering 0.3° in ω . Data were corrected for absorption by using a multiscan method applied with the SADABS program.³⁵ The structures of the compounds were solved by the Patterson method. Refinement, by full-matrix least-squares on F^2 with SHELXL97,³⁶ was similar for all complexes, including isotropic and subsequently anisotropic displacement parameters. The hydrogen atoms were observed or calculated and refined freely or using a restricted riding model. The hydride ligand was observed in the difference Fourier maps but refined with the same Os-H bond length. In the last cycles of refinement 0.5 molecule of toluene and water were observed in the asymmetric unit of **5**.

Crystal data for **2**: $\text{C}_{24}\text{H}_{31}\text{Cl}_2\text{N}_3\text{OsP}_2$, M_w 676.70, orange, irregular block ($0.16 \times 0.10 \times 0.04$), monoclinic, space group $P2_1/n$, $a = 8.750(2)$ Å, $b = 18.705(5)$ Å, $c = 17.512(5)$ Å, $\beta = 96.759(4)^\circ$, $V = 2846.3(12)$ Å³, $Z = 4$, $D_{\text{calc}} = 1.579$ g cm⁻³, $F(000)$: 1368, $T = 105(2)$ K, $\mu = 4.793$ mm⁻¹; 32 647 measured reflections ($2\theta = 3\text{--}58^\circ$, ω scans 0.3°), 7009 unique ($R_{\text{int}} = 0.0944$); min./max. transm factors 0.623/0.831. Final agreement factors were $R_1 = 0.0509$ (5089 observed reflections, $I > 2\sigma(I)$) and $wR_2 = 0.1286$; data/restraints/parameters 7009/2/296; GoF = 1.055. Largest peak and hole 2.394 and -1.130 e/Å³.

Crystal data for **5**: $\text{C}_{24}\text{H}_{36}\text{Cl}_2\text{N}_3\text{OsP} \cdot 0.25\text{H}_2\text{O} \cdot 0.25\text{C}_7\text{H}_8$, M_w 686.17, red, plate ($0.14 \times 0.10 \times 0.01$), triclinic, space group $P\bar{1}$, $a = 9.2152(11)$ Å, $b = 16.7244(19)$ Å, $c = 18.191(2)$ Å, $\alpha = 91.582(2)^\circ$, $\beta = 99.521(2)^\circ$, $\gamma = 95.268(2)^\circ$, $V = 2750.6(6)$ Å³, $Z = 4$, $D_{\text{calc}} = 1.657$ g cm⁻³, $F(000)$: 1364, $T = 100(2)$ K, $\mu = 4.908$ mm⁻¹; 25 797 measured reflections (2θ : $3\text{--}58^\circ$, ω scans 0.3°), 12 960 unique ($R_{\text{int}} = 0.0588$); min./max. transm. factors 0.639/0.952. Final agreement factors were $R_1 = 0.0441$ (7439 observed reflections, $I > 2\sigma(I)$) and $wR_2 = 0.0907$; data/restraints/parameters 12960/4/598; GoF = 0.664. Largest peak and hole 1.498 and -1.201 e/Å³.

Acknowledgment. Financial support from the MICINN of Spain (project number CTQ2005-00656 and Consolider Ingenio 2010 CSD2007-00006) and the Diputación General de Aragón (E35) is acknowledged. F.J.F.-A. thanks the CSIC and the European Social Fund for funding through the I3P Program.

Supporting Information Available: Detailed X-ray crystallographic data (bond distances, bond angles, and anisotropic parameters) for **2** and **5** as CIF files. Orthogonal coordinates of the optimized theoretical structures. This material is available free of charge via the Internet at <http://pubs.acs.org>.

OM8007772

(35) Blessing, R. H. *Acta Crystallogr.* **1995**, *A51*, 33. SADABS: Area-detector absorption correction; Bruker-AXS: Madison, WI, 1996.

(36) SHELXTL Package v. 6.10; Bruker-AXS: Madison, WI, 2000. Sheldrick G. M. *Acta Crystallogr.* **2008** *A64*, 112.

(34) Pople, J. A., et al. *Gaussian 03*, Revision B.05; Gaussian, Inc.: Wallingford, CT, 2004.